Pion-Exchange Contributions to Charge Densities of Closed-Shell Nuclei

J. W. Negele

Center for Theoretical Physics, Massachusetts Institute of Technology, Cambridge, Massachusetts 02139

and

D. O. Riska

Department of Physics, Michigan State University, East Lansing, Michigan 48823

The contribution to the nuclear charge density of the two-body pion-exchange charge operator is calculated for closed-shell nuclei from ^{12}C to ^{208}Pb using density-dependent Hartree-Fock wave functions.

Most meson-exchange effects on nuclear-charge form factors attain appreciable magnitude only for momentum transfer values much larger than 5 fm^{-1} and hence need not be taken into account when extracting charge densities from elastic-electron-scattering data. A notable exception is the lowest-order two-body pion-exchange charge operator, which in few-nucleon systems yields contributions comparable to those of the proton form factor for momentum transfers well below 5 fm^{-1}.[1-3]

This operator has the form

$$\rho(1,2) = \frac{g^2}{8m^3}[F_1{}^S(q^2)\vec{\tau}^1 \cdot \vec{\tau}^2 + F_1{}^V \tau_3{}^2]\frac{(\vec{\sigma}^1 \cdot \vec{q})(\vec{\sigma}^2 \cdot \vec{l})}{\mu^2 + l^2} + (1 \rightarrow 2).$$ (1)

Here $F_1{}^{S,V}$ are the nucleon isoscalar and isovector form factors [$F_1(0) = 1$], g is the pion-nucleon coupling constant ($g^2/4\pi = 14.5$), and μ and m are the pion and nucleon masses, respectively. The momentum of the exchanged pion is $\vec{l}$ and that of the virtual photon $\vec{q}$. The operator (1) may be derived by considering the difference between the relativistic expression for the pion-exchange amplitude for $\gamma NN \rightarrow NN$ and the corresponding expression obtained with the nonrelativistic one-pion-exchange potential.[4]

Since the operator (1) significantly reduces the discrepancy between the theoretical and empirical charge form factors for few-nucleon systems[1,3] it is important to investigate its effect on the charge densities of heavy nuclei as well. In this Letter we therefore calculate the matrix elements of (1) in closed-shell nuclei throughout the periodic table (^{12}C, ^{16}O, ^{40}Ca, ^{48}Ca, ^{90}Zr, and ^{208}Pb) using density-dependent Hartree-Fock wave functions.[5,6] Whereas we expect the mean-field approximation to be adequate for the heavier nuclei, the application to ^{12}C is uncertain because of its softness with respect to shape deformation and it would be unjustifiable for ^{4}He. Previously, only the rather special cases of ^{16}O and ^{40}Ca have been considered.[7,8]

In a general N,Z closed-shell nucleus, described by a determinantal wave function, the matrix element of the exchange charge operator (1) is

$$F_{II}(q) = -\frac{1}{Z}\frac{g^2}{2\pi^2}\frac{g}{m^3}\sum_{\alpha,\beta}F_{\alpha\beta}(q^2)\sum_{n_1 l_1 j_1}^{N_\alpha}\sum_{n_2 l_2 j_2}^{N_\beta}\int dr_1 r_1{}^2 \varphi_{n_1 l_1 j_1}{}^\alpha(r_1)\varphi_{n_2 l_2 j_2}{}^\beta(r_1) j_1(qr_1)$$

$$\times \int dr_2 r_2{}^2 \varphi_{n_1 l_1 j_1}{}^\alpha(r_2)\varphi_{n_2 l_2 j_2}{}^\beta(r_2)\sum_{ll'}G(l_1 l_2, j_1 j_2, ll')I_{ll'}(r_1,r_2).$$ (2)

Here the α,β sums are taken over nucleon species (n,p) and $N_{\alpha,\beta} = N,Z$. The function $I_{ll'}$ is defined as

$$I_{ll'}(r_1,r_2) = \frac{\mu\pi}{2(r_1 r_2)^{1/2}}\{\theta(r_1 - r_2)K_{l+1/2}(\mu r_1)I_{l'+1/2}(\mu r_2) - \theta(r_2 - r_1)I_{l+1/2}(\mu r_1)K_{l'+1/2}(\mu r_2)\}.$$ (3)

The form factors $F_{\alpha\beta}$ are defined by $F_{pp} = 2F_p{}^1$, $F_{pn} = F_{np} = 2(F_p{}^1 + F_n{}^1)$, and $F_{nn} = 2F_n{}^1$. Finally the coeffi-

cient G is defined

$$G(l_1 l_2, j_1 j_2, ll') = 6[l_1][l_2][j_1][j_2][l][l'] \begin{pmatrix} 1 & l & l' \\ 0 & 0 & 0 \end{pmatrix} \begin{pmatrix} l_1 & l' & l_2 \\ 0 & 0 & 0 \end{pmatrix}$$

$$\times \sum_{P=0}^{2} \sum_{\substack{d L L' \\ S S' J}} [d][P][L][L'][S][S'][J](-)^{l'+J+S+S'} \begin{pmatrix} 1 & l & d \\ 0 & 0 & 0 \end{pmatrix} \begin{pmatrix} l_1 & d & l_2 \\ 0 & 0 & 0 \end{pmatrix} \begin{Bmatrix} l' & l & l \\ 1 & P & d \end{Bmatrix} \begin{Bmatrix} L & L' & P \\ S' & S & J \end{Bmatrix}$$

$$\times \begin{Bmatrix} L & L' & P \\ l_1 & l_2 & d \\ l_2 & l_1 & d' \end{Bmatrix} \begin{Bmatrix} S & S' & P \\ \frac{1}{2} & \frac{1}{2} & 1 \\ \frac{1}{2} & \frac{1}{2} & 1 \end{Bmatrix} \begin{Bmatrix} l_1 & l_2 & L \\ \frac{1}{2} & \frac{1}{2} & S \\ j_1 & j_2 & J \end{Bmatrix} \begin{Bmatrix} l_1 & l_2 & L' \\ \frac{1}{2} & \frac{1}{2} & S' \\ j_1 & j_2 & J \end{Bmatrix}. \qquad (4)$$

Here we have used the notation $[l] = 2l + 1$. The sums over l, l' in (2) and d, L, L', S, S', J in (4) run over all allowed integer values leading to nonvanishing results.

From the form-factor contribution (2) we obtain the pion-exchange correction to the charge density as the Hankel transform

$$\rho_{ex}(r) = \int \frac{dq\, q^2}{2\pi^2} j_0(qr) F_{\Pi}(q). \qquad (5)$$

The integrals in Eq. (2) were performed numerically with density-dependent Hartree-Fock wave functions[5,6] computed on a 0.1-fm mesh. The computational procedure was tested by substituting oscillator wave functions to reproduce the results for ^{4}He, ^{16}O, and ^{40}Ca obtained in Ref. 8 with an entirely different technique.
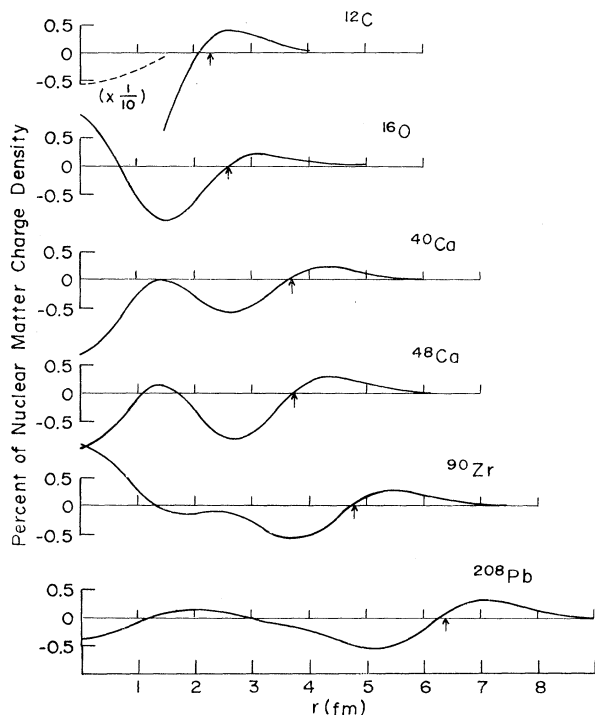
FIG. 1. Charge-density correction $\rho_{ex}(r)$ expressed in percent of the proton density in nuclear matter.

The calculated charge-density corrections are shown in Fig. 1, where the correction in percent of the proton density in nuclear matter [$100\rho_{ex}(r)/0.075$ fm^3] is plotted against the radius r. Qualitatively, the corrections resemble the result of a simple smearing of the original charge distribution over a range of order $1/\mu$. Outside the half-density radii (indicated by arrows in Fig. 1) the density is increased and immediately inside it is correspondingly decreased. The shape of the correction in the surface region is similar for all nuclei considered. The 0.08-fm^2 increase in $\langle r^2 \rangle$ found for ^{208}Pb is reasonably close to the Fermi-gas estimate of 0.05 fm^2 in Ref. 8. For the nuclei ^{16}O and ^{90}Zr, the exchange corrections tend to fill in the minima in the central nucleon density. In the case of the other nuclei, for which the nucleon density has central peaks, the exchange correction serves to diminish those peaks.

Because the main feature of the exchange correction is a smoothing of the nuclear charge distribution, the effect is qualitatively similar to a purely nuclear many-body correction to the mean-field approximation. Thus it is not possible to argue that discrepancies of this general structure between theory and experiment are necessarily attributable to pion-exchange effects. Yet it is nevertheless gratifying that the calculated exchange corrections do tend to systematically reduce the discrepancies between theory and experiment.

Since the mean-field approximation should be most reliable for ^{208}Pb, we exhibit a detailed comparison between theory and experiment for that nucleus in Fig. 2. The percent deviation of the experimental cross-section values[9-11] from those calculated in the mean-field approximation with corrections for nucleon form factors and the spin-orbit interaction[12] is denoted by the displacement of the error bars from the horizontal axis. The deviation from the calculated values after inclusion of the exchange effect is indicated by the
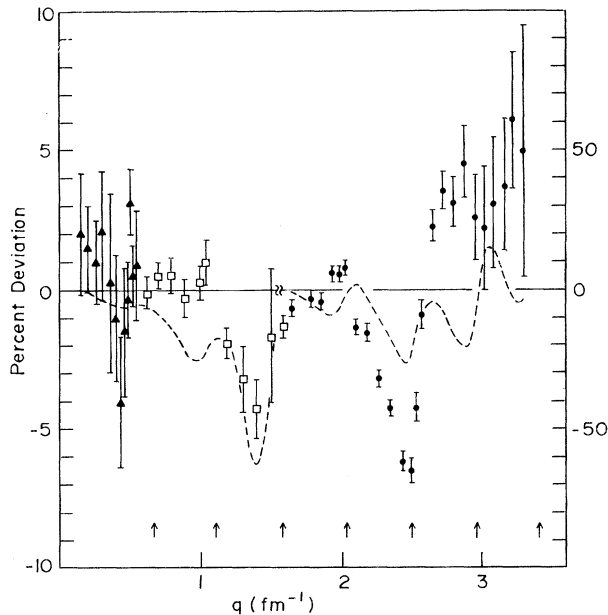
FIG. 2. Percent deviation of experimental elastic cross sections for ^{208}Pb. Note that different scales are used above and below 1.5 fm^{-1}. ▲-Ref. 9, 52.9 MeV; □-Ref. 10, 119 and 119.5 MeV; ●-Ref. 11, 501.6 MeV.

displacement from the dashed line. The exchange correction is thus large compared to the experimental errors and taking it into account reduces the χ^2 for the total supply of available data[13] from 4822 to 2683.

Because of the large distortion and significant contribution of the imaginary amplitude near the diffraction minima (indicated by arrows in Fig. 2), there is no simple way to compare form factors directly with data. The crucial features of the exchange corrections are, however, adequately conveyed by the fractional change induced at the diffraction maxima. For the nuclei other than ^{208}Pb, we give this information in Table I. A comparison with mean-field predictions in the

literature[5,14] shows that for these other nuclei the exchange correction also systematically reduces the discrepancies with experiment.

The present calculation of exchange charge effects is only exploratory and the results are subject to a number of uncertainties. The magnitude of the pion-exchange effect would be somewhat reduced by introduction of hadronic form factors at the πN vertices. Since the range of such form factors would most certainly not exceed a value of the order $1/m \simeq 0.15$ fm,[15] the resulting reduction would be very small.[16] On the other hand, the exchange charge effect would be enhanced somewhat by taking into account the two-body ρ-meson exchange effect. The magnitude of this enhancement does, however, depend sensitively on the assumed values for the ρN coupling constants and the range of the ρN-vertex form factors. The net result of introducing ρ-meson exchange and meson-nucleon form factors is, in fact, rather close to that obtained with the bare-pion-exchange operator (1) alone.[16] We thus believe the present estimates of ρ_{ex} to be representative and not likely to be drastically altered by the inclusion of other exchange effects.

From this investigation we conclude that, as in light nuclei, exchange contributions are definitely significant in heavy nuclei at the present level of experimental resolution. Any serious program of improving the many-body approximations for the nuclear density must thus necessarily be accompanied by quantitative treatment of meson exchange effects.

TABLE I. Calculated values of the momentum transfer in inverse femtometers and percent change of charge form factor due to exchange contributions (in parentheses) at the Nth diffraction maximum.

N	^{12}C	^{16}O	^{40}Ca	^{48}Ca	^{90}Zr
1	2.2 (+ 22)	1.9 (− 1)	1.4 (− 1)	1.4 (− 2)	1.1 (− 1)
2	3.6 (+ 17)	3.3 (+ 82)	2.3 (− 4)	2.2 (− 2)	1.8 (− 3)
3			3.2 (+ 57)	3.2 (+ 44)	2.4 (− 4)
4			3.9 (+ 21)	3.7 (+ 39)	3.1 (+ 30)
5					3.6 (+ 36)

[1]W. Kloet and J. Tjon, Phys. Lett. 49B, 419 (1974).

[2]A. D. Jackson, A. Lande, and D. O. Riska, Phys. Lett. 55B, 23 (1975).

[3]J. Borysowicz and D. O. Riska, Nucl. Phys. A254, 301 (1975).

[4]The form factors F_1 in (1) are a consequence of using pseudovector πN coupling; with pseudoscalar coupling they would be replaced by the corresponding magnetic form factors G_M.

[5]J. W. Negele, Phys. Rev. C 1, 1260 (1970).

[6]J. W. Negele and D. Vautherin, Phys. Rev. C 5, 1472 (1972).

[7]M. Gari, H. Hyuga, and J. G. Zabolitzky, Nucl. Phys. A271, 365 (1976).

[8]M. Radomski and D. O. Riska, Nucl. Phys. A274, 428 (1976).

[9]G. J. C. VanNiftrik, Nucl. Phys. A131, 574 (1969).

[10]H. Euteneur, J. Friedrick, and N. Voegler, Phys. Rev. Lett. 36, 129 (1976).

[11]B. Frois et al., Phys. Rev. Lett. 38, 152, 576(E) (1977).

[12]W. Bertozzi, J. Friar, J. Heisenberg, and J. W. Negele, Phys. Lett. 41B, 408 (1972).

[13]J. L. Friar and J. W. Negele, in Proceedings of the 1977 Bates Linac Summer Study, edited by A. Bernstein (unpublished).

[14]J. W. Negele, Phys. Rev. Lett. 27, 1291 (1971).

[15]J. W. Durso, A. D. Jackson, and B. J. Verwest, Nucl. Phys. A282, 404 (1977).

[16]D. O. Riska and M. Radomski, Phys. Rev. C 16, 2105 (1977).

Resonant Backward-Angle Heavy-Ion Elastic Scattering

M. R. Clover, R. M. DeVries, R. Ost, N. J. A. Rust,[a] R. N. Cherry, Jr.,[b] and H. E. Gove

Nuclear Structure Research Laboratory, University of Rochester, Rochester, New York 14627

(Received 21 November 1977)

We observe strong structure in the excitation functions of ^{12}C + ^{28}Si backward-angle scattering. Angular distributions at the peaks of the elastic excitation function are of the form $P_J^2(\cos\theta)$ [approximately $J = 15$ ($E_{c.m.} = 23.3$ MeV), $J = 18$ ($E_{c.m.} = 26.0$ MeV), and $J = 18$ ($E_{c.m.} = 30.2$ MeV)]. These results appear to be inconsistent with existing theoretical descriptions of anomalous backward-angle heavy-ion elastic scattering in this mass region.

Systematic studies of ^{16}O + ^{28}Si elastic scattering[1] and ^{12}C + ^{28}Si elastic scattering[2,3] have shown anomalous midenergy ($E_{c.m.} \sim 30$ MeV), midangle ($40° \lesssim \theta_{c.m.} \lesssim 90°$) structure. Braun-Munzinger *et al.*[4] have measured the elastic angular distribution for the ^{16}O + ^{28}Si system out to $\theta_{c.m.} = 180°$ and found large oscillatory cross sections. Theoretical interpretations of these results have included Regge poles,[4] a variable-moment-of-inertia rotational band,[5] and surface transparent optical potentials with coupled-channel effects.[6] These and other interpretations are presented elsewhere.[7] We have measured the backward-angle angular distribution of the system ^{12}C + ^{28}Si over the energy range (17.5 MeV $\lesssim E_{c.m.} \lesssim$ 33 MeV). Our observations are apparently inconsistent with all of the existing theories of the oscillatory backward-angle enhancements of ^{12}C + ^{28}Si and ^{16}O + ^{28}Si elastic scattering.

The ^{28}Si beam of the University of Rochester MP tandem was used to bombard carbon and beryllium foils of an approximate thickness of 100 μg/cm^2. The elastically scattered C or Be ions were detected at forward angles corresponding to c.m. angles (in the ^{28}Si target system) between 120° and 175°. Complete mass, Z, and charge-state identification of the reaction products was provided by the Enge split-pole Rochester heavy-ion detector system.[8] Several angles could be measured simultaneously because the angle of incidence is determined for each event. Absolute normalizations were obtained by monitoring the scattering from a thin layer of Au which was evaporated on the targets.

We have measured backward angular distributions for the ^{12}C + ^{28}Si at 28 energies in the range 17.5 MeV $\lesssim E_{c.m.} \lesssim$ 33 MeV. At each incident energy the data are averaged over about $\pm$ 200 keV because of the thickness of the target. Examples of the data are shown in Fig. 1. At all energies a rise in cross section is seen as $\theta_{c.m.}$ increases. The observed ratio of $\sigma/\sigma_R \sim 10^{-2}$ is about two orders of magnitude higher than expected with use of systematic potentials of Refs. 1 and 2. Furthermore, at certain c.m. energies the data show regular oscillations which can be fitted with the square of a Legendre polynomial. These features were also seen in the ^{16}O + ^{28}Si system.[4] However, at intermediate energies the oscillations in the angular distributions are irregular or weak and have a lower overall magnitude. This latter feature is best observed in Fig. 2